

HOSTED BY



ELSEVIER

Contents lists available at ScienceDirect

## Electronic Journal of Biotechnology



# Photo-fermentational hydrogen production of *Rhodobacter* sp. KKU-PS1 isolated from an UASB reactor



Thitirut Assawamongkholisiri<sup>a</sup>, Alissara Reungsang<sup>a,b,\*</sup>

<sup>a</sup> Department of Biotechnology, Faculty of Technology, Khon Kaen University, Khon Kaen 40002, Thailand

<sup>b</sup> Research Group for Development of Microbial Hydrogen Production Process from Biomass, Khon Kaen University, Khon Kaen 40002, Thailand

## ARTICLE INFO

## Article history:

Received 6 November 2014

Accepted 19 February 2015

Available online 2 April 2015

## Keywords:

nifD

nifH

Photo fermentation

Purple-non-sulfur bacteria

## ABSTRACT

**Background:** In this study, the detection of nifH and nifD by a polymerase chain reaction assay was used to screen the potential photosynthetic bacteria capable of producing hydrogen from five different environmental sources. Efficiency of photo-hydrogen production is highly dependent on the culture conditions. Initial pH, temperature and illumination intensity were optimized for maximal hydrogen production using response surface methodology with central composite design.

**Results:** *Rhodobacter* sp. KKU-PS1 (GenBank Accession No. KC478552) was isolated from the methane fermentation broth of an UASB reactor. Malic acid was the favored carbon source while Na-glutamate was the best nitrogen source. The optimum conditions for simultaneously maximizing the cumulative hydrogen production ( $H_{max}$ ) and hydrogen production rate ( $R_m$ ) from malic acid were an initial of pH 7.0, a temperature of 25.6°C, and an illumination intensity of 2500 lx.  $H_{max}$  and  $R_m$  levels of 1264 ml H<sub>2</sub>/l and 6.8 ml H<sub>2</sub>/L-h were obtained, respectively. The optimum initial pH and temperature were further used to optimize the illumination intensity for hydrogen production. An illumination intensity of 7500 lx gave the highest values of  $H_{max}$  (1339 ml H<sub>2</sub>/l) and  $R_m$  (12.0 ml H<sub>2</sub>/L-h) with a hydrogen yield and substrate conversion efficiency of 3.88 mol H<sub>2</sub>/mol<sub>malate</sub> and 64.7%, respectively.

**Conclusions:** KKU-PS1 can produce hydrogen from at least 8 types of organic acids. By optimizing pH and temperature, a maximal hydrogen production by this strain was obtained. Additionally, by optimizing the light intensity,  $R_m$  was increased by approximately two fold and the lag phase of hydrogen production was shortened.

© 2015 Pontificia Universidad Católica de Valparaíso. Production and hosting by Elsevier B.V. All rights reserved.

## 1. Introduction

Alternative energy is one of the solutions to environmental problems such as global warming and climate change. Among the alternative energies available, hydrogen has received increasing attention due to its environmentally friendly characteristics and high energy content [1]. Biologically, hydrogen can be produced by dark fermentation, photo-fermentation, biophotolysis, and microbial electrolysis [2]. Dark fermentation utilizes various substrates to produce hydrogen at a high rate in which volatile fatty acids (VFAs) are produced as the main soluble metabolites. VFAs can accumulate in the effluent that requires additional treatment before being released into the environment. In addition, the imbalance between acidogens and methanogens results in digestion failure due to the accumulation of VFAs with an associated drop in pH [3]. However, VFAs can be utilized by photosynthetic bacteria to produce hydrogen with a high hydrogen yield (HY) (i.e., approximately 50% of theoretical

value (4–6 mol H<sub>2</sub>/mol<sub>glucose</sub>)) [4,5]. For this reason, a search for microorganisms that efficiently produce hydrogen from VFA containing wastes is needed. Apart from reducing COD loading, hydrogen can also be produced from these VFA containing wastes. Examples of wastes containing VFAs are those from the wineries, distilleries and beverage industries [6,7] as well as the effluent from hydrogen production process by dark fermentation.

Among the bio-hydrogen producers, the purple non-sulfur photosynthetic bacteria (PNSB) are regarded as effective in producing hydrogen from different kinds of substrates containing VFAs and sugar [8]. *Rhodobacter sphaeroides* KKU-PS5 used malate [9] and *R. sphaeroides* KD131 used succinate to produce hydrogen [10]. Lactate was reported as the substrate for hydrogen production by *R. sphaeroides* KD131 [11]. Acetate and butyrate were used by *R. sphaeroides* O.U.001 [12] and *Rhodospseudomonas palustris* WP3-5 [13] to produce hydrogen, respectively. Mixed VFAs consisting of acetate, propionate and butyrate were used by *Rhodospseudomonas capsulata* to produce hydrogen [14]. Additionally, the effluent from dark fermentation of hydrogen was used as a substrate to produce hydrogen by *R. sphaeroides* NRRL-B1727 [15] and *R. sphaeroides* RS [16]. Not only VFAs but also other carbon sources such as glucose were used by *palustris* Rp. CQK 01 to produce hydrogen

\* Corresponding author.

E-mail address: alissara@kku.ac.th (A. Reungsang).

Peer review under responsibility of Pontificia Universidad Católica de Valparaíso.

[17]. PNSB are widely distributed in aquatic and wastewater environments [18,19,20]. They can be isolated from the environment using conventional enrichment techniques. However, these methods are time-consuming, tedious, and require a large number of samples. In order to overcome these limitations, application of a molecular biology technique, the polymerase chain reaction (PCR), was used in this study to detect the potential genes in the isolates responsible for hydrogen production. Hydrogenase is responsible for the production of hydrogen from organic acids in dark fermentation, while nitrogenase is responsible for the production of hydrogen by PNSB [8,21,22]. Mo nitrogenase consists of a nitrogenase iron (Fe) protein, called dinitrogenase reductase (or nifH) and a nitrogenase molybdenum-iron (MoFe) protein known as dinitrogenase, which consists of two subunits denoted alpha (or nifD) and beta (or nifK) [23,24]. In this study, we employed the PCR assay developed by Tan et al. [25] for the detection of nifH and nifD. This was done to screen for potential PNSB capable of producing hydrogen. This PCR assay offers a quick and efficient pre-identification of PNSB hydrogen producers [25].

Photo-hydrogen production strictly depends on operating/operational conditions. Environmental factors such as pH, temperature and illumination intensity have the greatest impact on hydrogen production [21,26,27]. The pH influences the ionic concentration at the active sites and enzyme activity. Temperature affects cell synthesis, HY, hydrogen production rate (HPR) and substrate conversion efficiency [26]. PNSB require energy from light to use in ATP synthesis for cell growth and hydrogen production [28,29]. Additionally, light intensity affects the irradiation area, cell concentration and surface-to-volume ratio in the bioreactor [30]. For these reasons, the environmental factors including pH, incubation temperature, and illumination intensity needed to be optimized before practical use of the isolates and to maximize hydrogen production.

To facilitate determination of the optimum conditions, a statistical experimental design by response surface methodology (RSM) with central composite design (CCD) was used to overcome the disadvantages of the conventional one-factor-at-a-time method [31,32]. RSM with CCD reduces the load of experimental measurements, saves both time and cost [33,34], as well as minimizes errors in determining the effects of parameters. It is also capable of determining interactive effects among the treatment variables [31,35].

In this research, we attempted to isolate PNSB capable of producing hydrogen from different environmental sources using the PCR assay to detect nifH and nifD genes. Subsequently, the newly isolated strains were identified, phylogenetically classified, and screened for carbon and nitrogen utilization. The key culture conditions affecting bio-hydrogen production included initial pH and incubation temperature. These variables were optimized by RSM with CCD in order to achieve maximal hydrogen production and HPR. Furthermore, the effects of illumination intensity on hydrogen production were investigated at the optimum initial pH and incubation temperature. The isolate obtained from this study can potentially be used to treat VFA containing wastes using an integrated system of dark-fermentative bacteria and PNSB.

## 2. Materials and methods

### 2.1. Source of microorganisms

Hydrogen-producing PNSB were isolated from aquatic and wastewater treatment facilities. Samples were taken from the following three aquatic environments: East Sri-Than Lake (EST), Khon Kaen University, Khon Kaen, Thailand; West Sri-Than Lake (WST), Khon Kaen University, Khon Kaen, Thailand; and Songkhla Lake (SK), Phatthalung, Thailand. Additionally, four samples from wastewater treatment facilities were collected from the stabilization pond of a pig farm (SPP), Khon Kaen, Thailand; the cesspool of a cassava starch plant (CCS) Kalasin, Thailand; the facultative pond of a wastewater

treatment plant (FPW), Khon Kaen University, Khon Kaen, Thailand; and the methane fermentation broth of an upflow anaerobic sludge blanket (UASB) reactor in our laboratory.

### 2.2. Isolation of the microorganisms

PNSB were enriched and isolated by successive anaerobic cultivation under continuous illumination. Briefly, approximately 2 mL of each sample was inoculated into 18 mL of a basal medium which consisted of 2 g/L of DL-malic acid as a carbon source, 0.36 g/L of sodium glutamate as a nitrogen source, and 1 mL/L of trace elements [36]. The basal medium consisted of 0.5 g/L of  $\text{KH}_2\text{PO}_4$ , 0.4 g/L of  $\text{MgSO}_4 \times 7\text{H}_2\text{O}$ , 0.4 g/L of NaCl, 0.05 g/L of  $\text{CaCl}_2 \times 2\text{H}_2\text{O}$ , and 1.0 g/L of yeast extract. The trace elements consisted of 68.2 mg/L of  $\text{ZnCl}_2$ , 72.7 mg/L of  $\text{MnSO}_4 \times \text{H}_2\text{O}$ , 62 mg/L of  $\text{H}_3\text{BO}_3$ , 190 mg/L of  $\text{CoCl}_2 \times 6\text{H}_2\text{O}$ , 17.04 mg/L of  $\text{CuCl}_2 \times 2\text{H}_2\text{O}$ , 23.77 mg/L of  $\text{NiCl}_2 \times 6\text{H}_2\text{O}$ , 62.76 mg/L of  $\text{Na}_2\text{MoO}_4 \times 2\text{H}_2\text{O}$ , and 5.24 mg/L of  $\text{EDTA-Na}_2 \times 2\text{H}_2\text{O}$ . The pH of the medium was adjusted to 6.8 with the addition of NaOH pellets before autoclaving. Enrichment of the culture was conducted anaerobically at room temperature ( $32 \pm 2^\circ\text{C}$ ) under an illumination intensity of 2500 lx using light-emitting diode (LED) lamps (E27 Corn-1205, epiStar). Samples were horizontally shaken at 150 rpm. After 48 h of incubation, 2 mL of culture was transferred into another 18 mL of the basal medium. After three cycles of subculture, a single loop of the liquid culture was streaked onto basal medium agar plates (1.5% w/v agar) and incubated in an anaerobic jar under lighted conditions. After 7 d of incubation, red or pink colonies were selected and re-streaked three times. In this way, pure cultures were obtained. Each putative PNSB strain was transferred into serum bottles containing basal medium and incubated as described above.

### 2.3. DNA extraction and amplification of nifH and nifD genes by PCR

Total genomic DNA was extracted from 2 mL cultures generated anaerobically under continuous illumination at 2500 lx for 2 d. The total genomic DNA of selected isolates was extracted using the method described by Tan et al. [25]. PCR amplification of 16S rDNA was performed using the same conditions for all of the strains. The specific primers for the detection of the nifH and nifD genes in the genome of *palustris* Rp. (GenBank NC005296) were designed by Tan et al. [25]. The nifH forward primer NH1 (5'-ACT CCA CCC GTC TGA TCC TC-3') and nifH reverse primer NH2 (5'-CCG AGC ACG TCA TAG GAGAC-3') target a fragment of 253 bp which corresponded to the genomic location, 5,205,363 - 5,205,615. The nifD forward primer ND1 (5'-TGC TAC CGC TCG ATG AAC TA-3') and nifD reverse primer ND2 (5'-AAC CCG TCG TAG CCA TGA TA-3') target fragment of 545 bp which corresponded to location 5,203,390 - 5,203,934. PCR amplification was performed in 25  $\mu\text{L}$  aliquots containing 0.5  $\mu\text{L}$  of the DNA template, 1.0  $\mu\text{L}$  of primers (25  $\mu\text{M}$ ), 12.5  $\mu\text{L}$  of 2XPCR Master Mix #K0171 (Fermentas), and 11.0  $\mu\text{L}$  of distilled water. The PCR was carried out on a  $P \times 2$  thermal cycler (Thermo IEC Inc., Milford, MA, USA) following the method of Tan et al. [25]. Separation of the PCR products was achieved by agarose gel electrophoresis for 25 min at 90 V on a 0.8% (w/v) agarose gel in 1XTBE (Tris-borate EDTA) buffer. The gel was stained with ethidium bromide for 15 min and visualized on a UV transilluminator (Dolphin-Doc., Wealtec., Taiwan).

### 2.4. Strain identification and phylogenetic analysis

The 16S rRNA gene sequences were amplified by PCR using a universal primer set composed of the forward primer PA (5'-AGA GTT TGA TCC TGG CTC AG-3'), corresponding to positions 19–38. The reverse primer PH (5'-AAG GAG GTG ATC CAG CCG CA-3'), corresponding to positions 1541–1561 was also used [37]. The PCR protocol followed the method of Khamtib et al. [38]. The PCR products

were purified using a gel extraction method and sequenced using the BigDye® Terminator cycle sequencing kit, Version 3.1 (1st BASE Laboratories SdnBhd, Seri Kembangan, Malaysia) in accordance with the manufacturer's instructions. The partial 16S rRNA gene sequences were matched using DNA Baser Version 4.12 and identified by searching in GenBank using BLAST tools [39]. Subsequently, the sequences of reference microorganisms obtained from GenBank were aligned using Clustal X [40]. A phylogenetic tree was created to assess evolutionary distance using the neighbor-joining method [41]. Bootstrapping analysis [42] of 1000 re-samplings was performed to measure the confidence of the tree topologies using Mega 4 Version 4.0.2.

## 2.5. Bio-hydrogen production of the isolated PNSB strains using different carbon and nitrogen sources

The capacity of the KKU-PS1 strain to utilize different carbon and nitrogen sources for bio-hydrogen production was investigated in batch fermentation. The different carbon sources tested included malate, acetate, butyrate, succinate, propionate, formic acid, citrate, glucose, fructose, arabinose, sucrose, ethanol, methanol, glycerol, and D-mannitol at a concentration of 2 g/L, with 0.36 g/L (2 mM) of Na-glutamate as a nitrogen source. The concentration of 2 g/L of carbon was tested because it is a suitable concentration for the formation of total VFAs in hydrogen production by *Rhodobacter* sp. [13,43]. The capability of the KKU-PS1 strain to produce hydrogen using different nitrogen sources was examined. The experiments were conducted at a concentration of 2 mM of organic nitrogen (Na-glutamate) and inorganic nitrogen (ammonium sulfate) with a 2 g/L of DL-malic acid as the carbon source. Two micromolar of Na-glutamate was reported as the optimum nitrogen concentration for obtaining maximal hydrogen production by *R. sphaeroides* O.U.001 [12]. Therefore, a nitrogen concentration of 2 mM was used to test the capability of the KKU-PS1 strain in producing hydrogen. All of the experiments were performed in 60 mL serum bottles with a working volume of 40 mL. The fermentation broth contained 36 mL of sterile hydrogen production medium (HPM) and 10% (v/v) inoculum (cell concentrations of  $10^6$ – $10^7$  cells/mL). The HPM consists of 2.0 g/L of DL-malic acid, 0.5 g/L of Na-glutamate, 3.9 g/L of  $\text{KH}_2\text{PO}_4$ , 2.8 g/L of  $\text{K}_2\text{HPO}_4$ , 0.2 g/L of  $\text{MgSO}_4 \times 7\text{H}_2\text{O}$ , 0.01 g/L of  $\text{Na}_2\text{MO}_4 \times 2\text{H}_2\text{O}$ , and 2 mL/L of a stock solution of 5 g/L  $\text{FeSO}_4$  (Fe-EDTA complex). The initial pH of the HPM was adjusted to 7.0 using either NaOH pellets or 4 M HCl. Trace elements were added as described above. The HPM medium was sterilized at 121°C for 15 min before being used in hydrogen production. All of the above tests were done under

anaerobic conditions. The bottles were closed with a rubber stopper and capped with an aluminum seal. Subsequently, the head space of the bottles was flushed with argon for 3 min. The serum bottles were incubated at 30°C, horizontally shaken at 150 rpm, and illuminated at an intensity of 2500 lx in an incubator shaker (WIS-10R, Wisd Laboratory Instruments, Korea) using LED lamps.

## 2.6. Optimization of initial pH and incubation temperature for bio-hydrogen production

### 2.6.1. Experimental design

RSM with CCD was applied to determine the major and interactive effects of two independent factors (Table 1) i.e., initial pH (6–8) and incubation temperature (22–38°C). The ranges of initial pH and temperature were chosen as the result of a literature search. Previous reports indicated that an initial pH of 7 was found to be optimal for both cell growth and hydrogen production in PNSB [10,44,45] while hydrogen cannot be produced at an initial pH of 5 [44,45]. Therefore, the initial pH tested in this study was in the range of 6–8. There were several temperature ranges for photo-hydrogen production by PNSB. For example, the temperature range hydrogen production by *Rhodobacter* sp. was between 31–36°C [31] and 27.5–32.5°C for *Rp. palustris* CQK 01 [17]. Thus, in order to cover the possible optimum temperature for hydrogen production by the KKU-PS1 strain, fermentation at 22–38°C was studied. Maximum cumulative hydrogen production ( $H_{\text{max}}$ ) and maximum hydrogen production rate ( $R_m$ ) were selected as the desirable responses in a batch culture. The statistical analysis and test factors of  $X_i$  were coded as  $x_i$  values according to the following [Equation 1]

$$x_i = (X_i - X_0) / \Delta X_i \quad [\text{Equation 1}]$$

where  $x_i$  is the coded value of the variable,  $X_i$  is the actual value of the independent variable,  $X_0$  is the actual value of  $X_i$  at the center point and  $\Delta X_i$  is the step change value. A quadratic model [Equation 2] [46] was used to optimize the key environmental factors.

$$Y_i = \beta_0 + \sum \beta_i x_i + \sum \beta_{ii} x_i^2 + \sum \beta_{ij} x_i x_j \quad [\text{Equation 2}]$$

where  $Y_i$  is the predicted response ( $H_{\text{max}}$  or  $R_m$ ),  $\beta_0$  is a constant,  $\beta_i$  is the linear coefficient,  $\beta_{ii}$  is the squared coefficient,  $\beta_{ij}$  is the interaction coefficient, and  $x_i$  is the variable. The response variables ( $H_{\text{max}}$  and  $R_m$ ) were fitted using a predictive polynomial quadratic equation [Equation 2] in order to correlate the response variable to the independent variables [47,48]. The test conditions were designed with experimental data.

**Table 1**

Central composite experimental design matrix defining initial pH ( $X_1$ ) and incubation temperature ( $X_2$ ) and result on maximum cumulative hydrogen production ( $H_{\text{max}}$ ) and maximum hydrogen production rate ( $R_m$ ).

Run	Initial pH ( $X_1$ )		Incubation temperature ( $X_2$ )		$H_{\text{max}}$ (mL $\text{H}_2$ /L)		$R_m$ (mL $\text{H}_2$ /L-h)		Incubation time (d)
	Code	Actual	Code	Actual (°C)	Observed	Predicted	Observed	Predicted	
1	0	7.0	0	30	1128	1124	5.1	5.0	12
2	-1	6.5	-1	26	1166	1299	4.6	4.8	14
3	-2	6.0	0	30	1106	1099	3.1	3.3	19
4	2	8.0	0	30	686	695	5.0	4.4	8
5	0	7.0	0	30	1100	1124	5.6	5.0	11
6	-1	6.5	1	34	977	856	3.5	3.3	14
7	1	7.5	1	34	783	645	3.1	3.8	13
8	0	7.0	0	30	1105	1124	5.3	5.0	12
9	0	7.0	0	30	1109	1124	4.8	5.0	13
10	0	7.0	2	38	182	310	1.9	1.9	7
11	1	7.5	-1	26	990	1106	4.4	5.4	12
12	0	7.0	0	30	1170	1124	5.1	5.0	12
13	0	7.0	-2	22	1338	1213	5.4	5.0	14

$H_{\text{max}}$ : maximum cumulative hydrogen production;  $R_m$ : maximum hydrogen production rate.

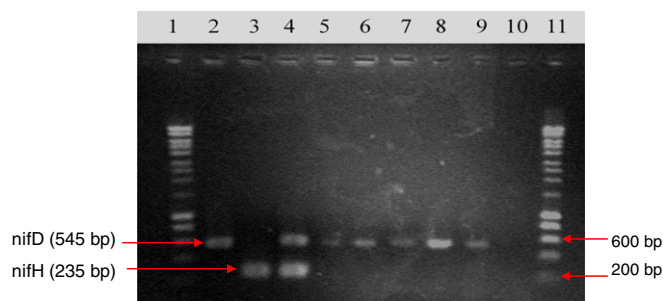


**Fig. 1.** The detection of *nifH* and *nifD* genes was used by monoplex and duplex PCR. Lanes 1 and 11: 100 bp marker; 2: 545 bp of *nifD*; 3: 235 bp of *nifH*; 4: duplex of *nifD* and *nifH*; 5–9: EST, WST, SK, SPP and UASB, respectively; 10: negative control.

Graphical analysis was performed using the statistical software, Design-Expert 7.0.0 Demo version (Stat-Ease, Inc., Minneapolis, MN, USA). A differentiation calculation was then used to predict the optimum values of the different factors simultaneously maximizing  $H_{\max}$  and  $R_m$  of the new isolate in batch fermentation.

### 2.6.2. Bio-hydrogen production from malic acid by the new isolate

Seed inocula were grown on basal medium in 60 mL serum bottles with a working volume of 40 mL, incubated at 30°C, horizontally shaken at 150 rpm and illuminated at a controlled light intensity of 2500 lx. After 48 h of incubation, 40 mL of culture was transferred to 360 mL of basal medium in 600 mL serum bottles. After 24 h of subculture, the culture was used as the inoculum of a batch experiment. Malic acid at a concentration of 2 mM was used as the model substrate to produce hydrogen in this study. This is because malic acid can be easily used as an energy source for supporting hydrogen formation by directly entering the tricarboxylic acid (TCA) cycle [10]. Na-glutamate at a concentration of 3 mM (0.5 g/L) was used as the nitrogen source. The cultures (mid-log phase) were harvested by centrifugation at 7000 rpm for 10 min. An initial cell concentration of 0.52 g cell dry weight (cdw)/L and 10% (v/v) inoculum was used for hydrogen production. To assess hydrogen production, the experiment was carried out in 300 mL serum bottles with a working volume of 180 mL. Hydrogen production was conducted at different initial pH values and incubation temperatures according to the design (Table 1). Using the predicted optimum conditions, the effects of illumination intensities of 2500, 5000, 7500 and 10,000 lx on hydrogen production by the PNSB isolates were

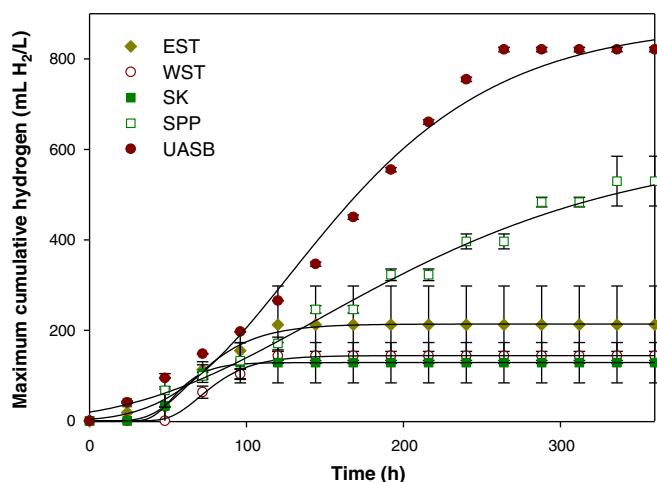


**Fig. 2.** Cumulative hydrogen production by PNSB strain EST, WST, SK, SPP, UASB grown on DL-malic acid.

**Table 2**  
Comparison PNSB strains on hydrogen production.

PNSB strains	HY (mol H <sub>2</sub> /mol malate)	Substrate degradation (%)	H <sub>max</sub> (mL H <sub>2</sub> /L)	R <sub>m</sub> (mL H <sub>2</sub> /L·h)	λ (h)	R <sup>2</sup>
EST	1.68	37.73	214	3.4	39	0.99
WST	1.77	18.39	144	2.9	52	0.99
SK	0.69	52.92	129	3.8	40	0.99
SPP	1.81	100.00	614	1.9	28	0.99
UASB	2.42	100.00	881	4.3	53	0.98

HY: hydrogen yield; H<sub>max</sub>: maximum cumulative hydrogen production; R<sub>m</sub>: maximum hydrogen production rate; λ: lag phase time; R<sup>2</sup>: regression coefficient; EST: East Sri-Tham Lake; WST: West Sri-Tham Lake; SK: Songkhla Lake; SPP: stabilization pond of a pig farm; UASB: upflow anaerobic sludge blanket reactor.

examined. All experiments were carried out under anaerobic conditions as described above.

### 2.7. Analytical methods

CDW was determined in four replicates using 7 mL culture samples. After filtration through a 0.45 μm membrane, the cells were washed with distilled water and dried at 85°C for 12 h (modified from Bianchi et al. [49]). The cell concentration was determined by measuring the absorbance at 660 nm with a UV-VIS Spectrophotometer (UVmini-1240, Shimadzu, Japan). An absorbance of 1.5 units was equivalent to 0.52 g<sub>cdw</sub>/L. The pH was measured using a digital pH meter (Sartorius, Germany).

The concentrations of VFAs (malic, acetic, butyric, propionic, lactic, formic, citric and succinic acids) in the liquid samples were analyzed using high performance liquid chromatography (HPLC) (Shimadzu LC-20AD, Shimadzu, Tokyo, Japan), employing refractive index (RI) and ultraviolet (UV) detectors with an Aminex HPX-87H column (Bio-Rad Laboratories, Hercules, CA, USA). The oven temperature was 45°C. The mobile phase was 5 mM H<sub>2</sub>SO<sub>4</sub> at a flow rate of 0.5 mL/min [50].

The volume of the biogas was measured by releasing pressure from each of the serum bottles using wetted glass syringes ranging in size from 5 to 50 mL [51]. The resulting biogas was collected every 12 h or 24 h for the analysis of its composition and hydrogen content using a Shimadzu GC-2014 apparatus equipped with a 2 m stainless steel column packed with Shin carbon (50/80 mesh), following Fangkum and Reungsang [52]. Preparation of the liquid samples prior to HPLC analysis was performed according to Saraphirom and Reungsang [53].

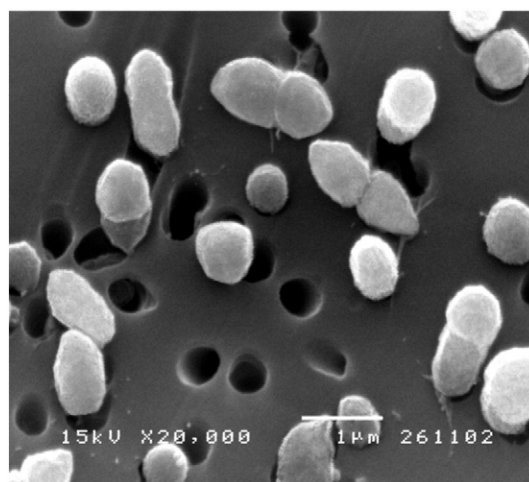


**Fig. 3.** Scanning electron microscopy (SEM) image of strain UASB under a JEOL JSM-5410LV electron microscope instrument operating at 15 kV and 20,000 X.

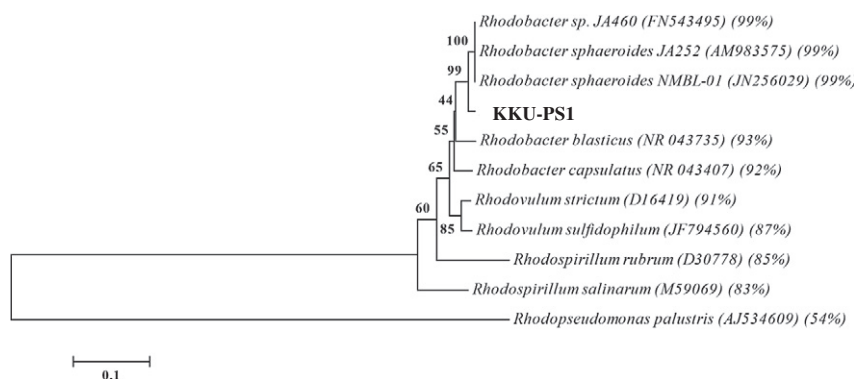


**Fig. 4.** Phylogenetic trees showing the relationship between strain KKU-PS1 and related species based on 16S rDNA sequences. The bar corresponds to a 10% difference in nucleotide sequence. The numbers shown next to the nodes indicate percent bootstrap values from 1000 iterations.

## 2.8. Calculations

Hydrogen gas production was calculated from head-space measurements of hydrogen composition and the total volume of hydrogen produced using a mass balance after each time interval [54]. The hydrogen production rate (HPR) (mL H<sub>2</sub>/L-h) was calculated by dividing H<sub>max</sub> (mL H<sub>2</sub>/L culture) by the incubation time (h). H<sub>max</sub> was calculated using a modified Gompertz equation [55].

The HY (mol H<sub>2</sub>/mol<sub>substrate</sub>) was calculated as the total amount of hydrogen (mol H<sub>2</sub>) divided by the amount of substrate consumed (mol<sub>substrate</sub>) on a molar basis. The amount of hydrogen was determined using the ideal gas law [Equation 3], where P = pressure (1 atm), V = H<sub>max</sub> (L H<sub>2</sub>/L culture), R = 0.0821 (L atm/K mol), and T = temperature (K) [56].

$$\text{Moles of hydrogen gas (n)} = PV/RT \quad [\text{Equation 3}]$$

The substrate conversion efficiency is a calculation of how much substrate has been converted for hydrogen production. The efficiency was determined by calculating the ratio of hydrogen produced to the

amount theoretically possible from stoichiometric conversion of the substrate [Equation 4] [57].

$$\text{Substrate conversion efficiency} = \frac{\text{mol H}_2 \text{ produced}}{\text{mol H}_2 \text{ theoretically possible}} \quad [\text{Equation 4}]$$

## 3. Results and discussion

### 3.1. Isolation of hydrogen-producing PNSB strains

Single red colonies isolated from the environmental samples were selected for further investigation. Red colonies indicated the presence of carotenoids and bacteriochlorophyll [44,58,59]. Most of the isolates were gram negative except those from CCS and FPW. These isolates were subsequently analyzed by PCR amplification to detect nifD and nifH genes before testing for hydrogen production ability.

The monoplex PCR targeting for each gene was individually performed to estimate the specificity of each primer. The primers for nifD and nifH yielded amplicons of 545 bp and 235 bp, respectively

**Table 3**

The effect of different carbon source on hydrogen production.

Carbon source	<i>Rhodobacter</i> sp. KKU-PS1		<i>R. sphaeroides</i> ZX-5		<i>R. sphaeroides</i> KKU-PS5		<i>R. sulfidophilum</i> P5	
	H <sub>2</sub> production	OD <sub>660nm</sub>	H <sub>2</sub> production	OD <sub>660nm</sub>	H <sub>2</sub> production	H <sub>2</sub> production	H <sub>2</sub> production	H <sub>2</sub> production
Organic acid	Malate	+	3.12	+	2.29	+	ND	
	Acetate	+	4.28	+	1.62	+	+	
	Butyrate	+	4.65	+	4.12	+	-	
	Succinate	+	2.60	+	2.44	+	±	
	Lactate	+	2.16	+	2.42	+	+	
	Propionate	+	2.31	+	2.45	-	-	
	Formic acid	-	1.37	ND	ND	ND	-	
	Citrate	-	0.52	ND	ND	-	-	
	Carbohydrate	Glucose	+	3.64	+	2.12	+	+
Fructose		+	3.47	+	2.41	+	+	
Arabinose		-	0.82	-	2.58	+	+	
Sucrose		-	1.61	+	2.05	-	+	
Other	NaCO <sub>3</sub>	+	1.54	ND	ND	ND	ND	
	Ethanol	-	0.94	-	1.87	-	ND	
	Methanol	-	0.69	ND	ND	ND	ND	
	Glycerol	-	2.84	ND	ND	ND	+	
	D-mannitol	+	4.38	+	2.95	+	-	
Reference		This study		[44]		[9]		[70]

Notes: + = presence of H<sub>2</sub> production; - = absence of H<sub>2</sub> production; ± = partially utilized and ND = not determined.

**Table 4**

Model coefficients estimated by multiple linear regressions (significance of regression coefficients).

Factors	$H_{\max}$ (mL $H_2$ /L)		$R_m$ (mL $H_2$ /L h)	
	Coefficient estimate	<i>p</i> -value	Coefficient estimate	<i>p</i> -value
Model	1123.57	0.0002	5.00	0.0152
$X_1$	-100.91	0.0223	0.27	0.1789
$X_2$	-225.62	0.0003	-0.79	0.0035
$X_1X_2$	-4.45	0.9428	-0.03	0.9268
$X_1^2$	-56.57	0.0581	-0.30	0.0592
$X_2^2$	-90.56	0.0085	-0.39	0.0199

Values of “Prob > F” less than 0.0500 indicate factor terms are significant.

$H_{\max}$ : maximum cumulative hydrogen production;  $R_m$ : maximum hydrogen production rate.

(Fig. 1, lanes 2 and 3). Then, a duplex PCR containing both primer sets (ND1 and 2, NH1 and 2) was done to simultaneously detect both genes (*nifD* and *nifH*) (Fig. 1, lane 4). *Rp. palustris* CGA009 was used as a positive control (Fig. 1, lanes 2, 3 and 4) while sterile water was used as a negative control to confirm that no amplicons were contaminated (Fig. 1, lane 10). The results from PCR amplification indicated that only five isolates (EST, WST, SK, SPP and UASB) contained the *nifD* gene (Fig. 1, lanes 5, 6, 7, 8 and 9) while the *nifH* gene was not observed. Even though these five isolates contained only the *nifD* gene, they still could efficiently produce hydrogen when DL-malic acid was used as a carbon source (Fig. 1 and Fig. 2). Theoretically, Mo nitrogenase activity involves a synergy between the Fe protein (*NifH*) and the MoFe protein (*NifDK*) (Danyal et al. [60]; Seefeldt et al. [61]; Hu and Ribbe [24]). The MoFe protein is an  $\alpha_2\beta_2$  heterotetramer composed of two types of metal clusters [62] that aggregate into large proteins enabling easy detection of *nifD*. This site is important for electron transfer activity and responsible for gene expression [61].

Among the five isolates, the strain isolated from the methane fermentation broth of an UASB reactor showed the highest  $H_{\max}$ , HY and  $R_m$  of 881 mL  $H_2$ /L, 2.42 mol  $H_2$ /mol<sub>malate</sub> and 4.3 mL  $H_2$ /L-h, respectively (Fig. 2 and Table 2). Thus, the UASB strain was further investigated for its hydrogen production capability. The possible reasons that the UASB strain exhibited the highest bio-hydrogen production potential might be due to its growth in a methane fermentation broth containing high concentrations of VFAs. The feedstock used to produce methane in the UASB was an acidic effluent (mainly butyric acid and propionic acid (data not shown)) coming from a sugarcane juice hydrogen fermentation process. Therefore, the UASB strain might have been able to adjust to the use of malic acid to produce hydrogen to a greater degree than isolates obtained from other environmental sources. Moreover, the difference in hydrogen production capability of the five isolates might have been due to the activities of the nitrogenase enzyme of each isolate. This speculation is

supported by the report of Xie et al. [63] who found that nitrogenase activity had a positive correlation to hydrogen production.

### 3.2. Characterization of the UASB strain

The UASB strain was gram-negative, with ovoid red colonies and dimensions of 0.88–1.21 × 0.58–0.62  $\mu\text{m}$ . Polar flagella were not observed. Cells were divided by binary fission. It could produce slime depending on the carbon source used and formed chains of cells (Fig. 3). Cultures were yellowish brown under anaerobic conditions and reddish brown in the presence of air. The absorption maxima of the UASB strain occurred at 471 and 505 nm due to the presence of carotenoids, and at 802 and 853 nm due to the presence of bacteriochlorophyll a [44,64]. The partial 16S rRNA gene sequence (1300 bp) of the UASB strain was deposited in GenBank with the Accession No. KC478552. The 16S rRNA gene analysis demonstrated that the UASB strain showed high similarity (99%) to *R. sphaeroides*. Therefore, this strain was named *Rhodobacter* sp. KKU-PS1. A phylogenetic tree (Fig. 4) revealed that KKU-PS1 strain was closely related to strains JA460, JA252 and NMBL-01. The KKU-PS1 strain showed the ability to grow on a wide variety of carbon sources (Table 3). The phenotypic characteristics of the KKU-PS1 strain were consistent with those of *R. sphaeroides* KKU-PS5 except that the KKU-PS5 strain could not utilize propionate although it could grow on arabinose (Table 3). Based on the range of carbon sources used, the KKU-PS5 strain can be considered a new strain within the species of *R. sphaeroides*.

### 3.3. Effect of carbon sources on bio-hydrogen production

KKU-PS1 was able to use all of the carbon sources tested for cell growth and was able to use ten of carbon sources tested for producing hydrogen (Table 3). This suggested that the KKU-PS1 strain had the potential to produce hydrogen and cells using VFAs and simple sugars as carbon sources. The highest cumulative hydrogen production of 881 mL  $H_2$ /L was achieved when malic acid was used as the carbon source (Table 2, Fig. 2), while maximum cell growth was obtained when butyrate was used as the carbon source (Table 3). The carbon source is usually the most important factor affecting the metabolism of photo-hydrogen production and cell synthesis [65,66]. The majority of carbon sources are utilized for cell synthesis. Only a few substrates can be used for photo-hydrogen production under suitable conditions [26]. Differences in hydrogen production utilizing different carbon sources were observed [67]. The discrepancy might be due to the variations in the electron transfer capabilities of cofactor compounds required for nitrogenase activity. The metabolic pathways of PNSB are different as well [26].

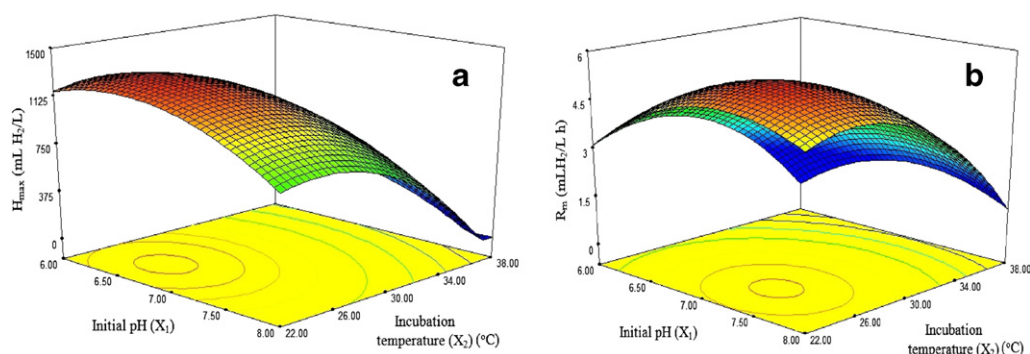


Fig. 5. Response surface plots showing the effect of initial pH and incubation temperature on  $H_{\max}$  (a) and  $R_m$  (b) from DL-malic acid by KKU-PS1.

**Table 5**  
Confirmation photo-hydrogen production experiment.

Run	Condition	initial pH	Temperature (°C)	H <sub>max</sub> (mL H <sub>2</sub> /L)		R <sub>m</sub> (mL H <sub>2</sub> /L ·h)		HY (mol H <sub>2</sub> /mol <sub>malate</sub> )
				Observed	Predicted	Observed	Predicted	
–	Optimum	7.0	25.6	1353	1264	6.8	5.4	3.92
2	Worst	6.5	26.0	1209	1299	5.3	4.8	3.50
1	Center	7.0	30.0	1118	1124	4.6	5.0	3.08
7	Height	7.5	34.0	838	645	4.1	3.8	2.28

H<sub>max</sub>: maximum cumulative hydrogen production; R<sub>m</sub>: maximum hydrogen production rate; HY: hydrogen yield.

### 3.4. Effect of nitrogen source on bio-hydrogen production

The KKU-PS1 strain produced large amounts of hydrogen with an organic nitrogen source, i.e., Na-glutamate (881 mL H<sub>2</sub>/L). With 2 mM of inorganic nitrogen, lower amounts of hydrogen were produced than with the same concentration of inorganic nitrogen, i.e., 530 mL H<sub>2</sub>/L of NH<sub>4</sub>Cl. This is due to direct solubilization of organic nitrogen into proteins or transfer into other nitrogenous cellular components [68]. Microorganisms require more a developed metabolism to use inorganic nitrogen for amino acid and protein production [67]. Additionally, a higher ammonium ion concentration in the form of NH<sub>4</sub>Cl instead of Na-glutamate inhibited nitrogenase activity of KKU-PS1 resulting in lower hydrogen production when NH<sub>4</sub>Cl was used as a nitrogen source [69].

### 3.5. Optimization of initial pH and incubation temperature on bio-hydrogen production and hydrogen production rate from malic acid by KKU-PS1

The effects of the initial pH (X<sub>1</sub>) and incubation temperature (X<sub>2</sub>) on two responses, i.e., H<sub>max</sub> (Y<sub>Hmax</sub>) and R<sub>m</sub> (Y<sub>Rm</sub>), were investigated. The regression models are shown in [Equation 5] and [Equation 6]:

$$Y_{H_{\max}} = -12419.63 + 3032.64X_1 + 298.76X_2 - 2.22X_1X_2 - 226.26X_1^2 - 5.66X_2^2 \quad [\text{Equation 5}]$$

$$Y_{R_m} = -76.32 + 17.58X_1 + 1.39X_2 - 0.02X_1X_2 - 1.18X_1^2 - 0.02X_2^2 \quad [\text{Equation 6}]$$

High values of the coefficient of determination (R<sup>2</sup>) of 0.9040 and 0.8205 for Y<sub>Hmax</sub> and Y<sub>Rm</sub>, respectively, indicated that the models accurately fit the experimental data. In the regressions, the coefficients for both factors, including the initial pH (X<sub>1</sub>) and incubation temperature (X<sub>2</sub>), were significant with a low *p*-value (*p* ≤ 0.05). Only incubation temperature (X<sub>2</sub>) affected the response of R<sub>m</sub>. However, no significant interaction was found between the initial pH and incubation temperature for H<sub>max</sub> and R<sub>m</sub> (X<sub>1</sub>X<sub>2</sub>) (*p* ≤ 0.05) (Table 4).

The observed and predicted values of initial pH and incubation temperature obtained from each condition are summarized in Table 1. The response surface plot representing the interaction effect of the initial pH and incubation temperature on H<sub>max</sub> based on [Equation 5]

is shown in Fig. 5a. The results indicated that an increase in the initial pH and incubation temperature led to a substantial decrease in H<sub>max</sub>. A peak value of 1304 mL H<sub>2</sub>/L at an initial pH of 6.6 and an incubation temperature of 25.1°C was observed. Three-dimensional response surfaces based on [Equation 6] were plotted in order to determine the optimum level of each variable and the effects of their interactions on R<sub>m</sub> (Fig. 5b). Over the experimental range, the highest predicted R<sub>m</sub> value of 5.5 mL H<sub>2</sub>/L-h was obtained at an initial pH of 7.3 and an incubation temperature of 26°C. R<sub>m</sub> increased following elevation of the initial pH from 6.00 to 7.3, but R<sub>m</sub> decreased when the initial pH was further increased from 7.3 to 8.0. Additionally, the incubation temperature showed a similar trend to that of the initial pH. R<sub>m</sub> increased when the incubation temperature was raised from 22 to 26°C, but decreased when the incubation temperature was greater than 26°C (Fig. 5b). When we optimized the conditions that simultaneously maximized H<sub>max</sub> and R<sub>m</sub> using [Equation 5] and [Equation 6], it was found that the maximum H<sub>max</sub> and R<sub>m</sub> values of 1264 mL H<sub>2</sub>/L and 5.4 mL H<sub>2</sub>/L-h, respectively, occurred at an initial pH of 7.0 and incubation temperature of 25.6°C. pH is a very critical factor influencing metabolism and HY of PNSB [70]. The active site and biochemical reaction characteristics of the nitrogenase enzyme, the enzyme responsible for hydrogen production in PNSB, were affected by its ionic form at different pH values in the culture medium [26,70].

Temperature has an important function of shifting the metabolic pathways towards photo-hydrogen production [21]. It affects cell synthesis, HY, hydrogen production rate and substrate conversion efficiency of photo-hydrogen producing bacteria [26,71]. The optimum initial pH of 7.0 in our study was found to be consistent with the other reports [10,27,44,71,72]. The optimum temperature in our study was slightly lower than other reports [10,73,74], where the optimum temperature range of *Rhodobacter* sp. was between 30 and 32°C. In contrast, Wang et al. [17] found that the optimal temperature for *Rp. palustris* CQK 01 was between 27.5 and 32.5°C.

### 3.6. Confirmation experiment

To reconfirm the adequacy of the model, batch fermentation experiments were conducted under the optimum, worst, median and high conditions (Table 5). The predicted values for simultaneously maximizing the H<sub>max</sub> and R<sub>m</sub> values, calculated from [Equation 5] and [Equation 6] under the optimum conditions were 1264 mL H<sub>2</sub>/L and

**Table 6**  
Comparison of hydrogen production by different microorganisms.

Microorganism	Malate con. (mM)	Conditions			H <sub>max</sub> (mL H <sub>2</sub> /L)	Substrate conversion efficiency (%)	Substrate degradation (%)	Incubation time (d)	Reference
		pH	Temp. (°C)	Illumination intensity					
<i>R. sphaeroides</i> KD131	30	7.0	30	6831 lx*	1190	22.2	93.1	3	[10]
<i>R. sphaeroides</i> NMBL-01	30	7.0	32 ± 2	1800 lx	2275	68.3	ND	15	[73]
<i>R. sphaeroides</i> RV	45	7.0	32	4000 lx	284	7.0	93.4	4	[74]
<i>R. sphaeroides</i> ZX-5	30	7.0	30 ± 1	5000 lx	3157	71.25	ND	3	[44]
<i>R. sphaeroides</i> O.U.001	7.5	6.8 ± 0.2	32 ± 2	932 lx*	650	44.9	ND	5	[75]
<i>Rhodobacter</i> sp. KKU-PS1	15	7.0	25.6	7500 lx	1339	64.7	100	8	This study

ND = not determined; H<sub>max</sub>: maximum cumulative hydrogen production.

\* = Illumination intensity was calculated (1 lx = 0.0161028 W/m<sup>2</sup>) [83].

**Table 7**  
Effect of illumination intensity on hydrogen production from DL-malic acid by KKU-PS1.

Light (lx)	H <sub>max</sub> (mL H <sub>2</sub> /L)	R <sub>m</sub> (mL H <sub>2</sub> /L-h)	λ (h)	R <sup>2</sup>	HY (mol H <sub>2</sub> /mol <sub>malate</sub> )	Incubation time (d)
2500	1353 ± 34	6.8 ± 0.4	57.1 ± 5.6	0.99	3.92	12
5000	1382 ± 38	8.1 ± 0.6	47.9 ± 5.6	0.99	3.95	10
7500	1339 ± 24	12.0 ± 0.8	40.9 ± 3.8	0.99	3.88	8
10,000	1258 ± 16	13.3 ± 0.9	39.8 ± 2.8	0.99	3.67	8

H<sub>max</sub>: maximum cumulative hydrogen production; R<sub>m</sub>: maximum hydrogen production rate; λ: lag phase time; R<sup>2</sup>: the determination coefficient; HY: hydrogen yield.

5.4 mL H<sub>2</sub>/L-h, respectively. These values were different from the observed values by only 6.5% and 21%, respectively. Hence, RSM with CCD was a useful tool to optimize photo-hydrogen production from DL-malic acid by KKU-PS1. The results under the optimum conditions in this study were compared to results from other experiments using DL-malic acid as a carbon source for hydrogen production (Table 6). The H<sub>max</sub> value obtained by the KKU-PS1 strain was comparable to that observed in *R. sphaeroides* KD131 [10], and greater than the levels found in *R. sphaeroides* RV [74] and *R. sphaeroides* O.U.001 [75]. However, the H<sub>max</sub> value of KKU-PS1 was lower than that obtained using *R. sphaeroides* NMBL-01 [73] and *R. sphaeroides* ZX-5 [44]. The KKU-PS1 strain could completely utilize DL-malic acid. This can be considered its distinguishing characteristic. The maximum malic utilization by other microorganisms was approximately 93% (Table 6). The difference in the H<sub>max</sub> and substrate conversion efficiency might be due to differences in illumination intensity, light source, medium composition and substrate concentrations used in each experiment. Additionally, it was clearly seen that the efficiencies of PNSB strains in producing hydrogen were different. These can be due to differences in mechanisms to transform carbon substrates of each PNSB strain. For example, if a few carbon substrates are used to produce the cells, a larger number of carbon substrates can be used to produce hydrogen. It was reported that a carbon substrate can be used in three ways, i.e., bacterial cell components, CO<sub>2</sub>/HCO<sub>3</sub><sup>-</sup> and non-volatile organic carbon compounds [76].

### 3.7. Effect of illumination intensity on bio-hydrogen production

The results show that illumination intensity plays an important role in photo-hydrogen production by the KKU-PS1 strain. Its R<sub>m</sub> increased with increasing illumination intensity. The maximum H<sub>max</sub> was obtained at 10,000 lx. H<sub>max</sub> slightly increased when the light intensity was increased from 2500 to 5000 lx and then decreased with further increases in light intensity. Additionally, an increase in light intensity from 2500 to 10,000 lx shortened the lag time (Table 7).

From these results, an optimum illumination intensity of 7500 lx gave the best conditions for the KKU-PS1 strain. Under these conditions, maximal values of H<sub>max</sub>, HY, and R<sub>m</sub> of 1339 mL H<sub>2</sub>/L, 3.88 mol H<sub>2</sub>/mol<sub>malate</sub>, and 12.0 mL H<sub>2</sub>/L-h were attained, respectively. Simultaneously, the shortest lag times of 40.9 h and 8 d resulted. The increase in H<sub>max</sub> and R<sub>m</sub> as light intensity increased from 2500 to 5000 lx which occurred because at a high illumination intensity, more ATP and reducing power were supplied to the photosynthetic system. These are essential for photo-hydrogen producing bacteria [77,78]. Large amounts of ATP (in the form of light energy) are required for nitrogenase activity to produce hydrogen and synthesize the cells. However, the results indicated that higher illumination intensity became a limiting factor for hydrogen production. This suggested that hydrogen production by the KKU-PS1 strain was saturated at an illumination intensity of 7500 lx. Light saturation might have occurred when the photosynthetic system provided excess ATP and Fd<sub>red</sub> compared to the capacity of nitrogenase enzyme [79]. Photo inhibition was observed in the studies of Kim et al. [80] who found that the light saturation occurred when light intensity was higher than 200 W/m<sup>2</sup> while Cai and Wang [70] reported that a light intensity of 6000 lx became an inhibiting factor for hydrogen production in *Rhodovulum sulfidophilum* P5.

In this study, LED were used as the light source because they have a suitable and specific wavelength range (770–920 nm) for bacteriochlorophyll a [81]. Moreover, LED light sources have several additional benefits, including lower energy consumption, lower heat generation, longer life expectancy and improved performance regarding photo-hydrogen production [27]. Other types of light sources used previous studies of photo-fermentation of hydrogen including halogen [65,80] and tungsten lamps [13,44,82].

### 3.8. Photo hydrogen production under the optimum conditions

Photo-hydrogen production of the KKU-PS1 strain in batch fermentation under the optimum conditions (initial pH 7.0, 25.6°C and 7500 lx) was investigated using DL-malic acid as the carbon

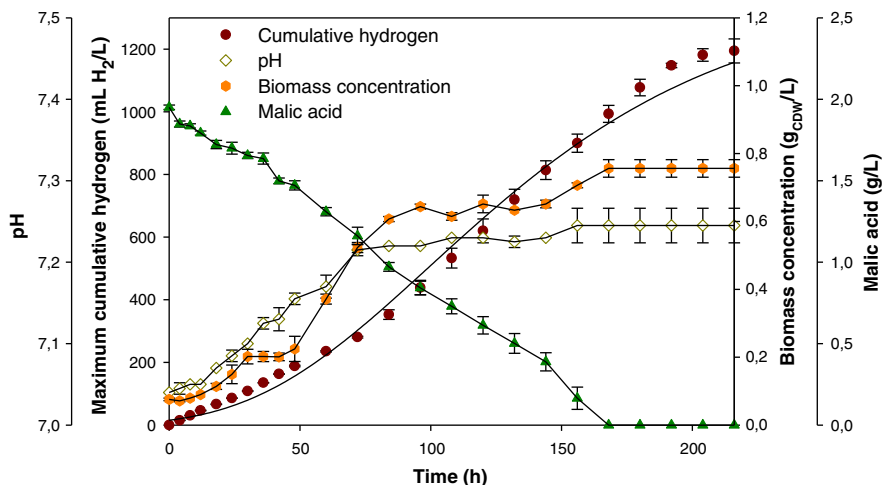


**Fig. 6.** Time course of photo hydrogen production during batch fermentation at optimum conditions of initial pH 7.0, 25.6°C and 7500 lx by KKU-PS1.



source. The biomass concentration of KKU-PS1 cells rapidly increased to 0.61 g<sub>CDW</sub>/L within 84 h of inoculation. Then, the biomass concentration increased slowly remaining within a range of 0.64–0.75 g<sub>CDW</sub>/L until the end of the photo-fermentation period (Fig. 6). Hydrogen was produced after a lag phase of about 32 h and ended at 216 h while the DL-malic acid was completely utilized by the end of photo-fermentation. When no carbon source was available (after 168 h) cell growth was at steady state. However, hydrogen was continuously produced until 216 h. Under optimum conditions, H<sub>max</sub>, R<sub>m</sub> and HY values were 1378 mL H<sub>2</sub>/L, 7.6 ml H<sub>2</sub>/L h, and 3.85 mol H<sub>2</sub>/mol<sub>malate</sub>, respectively, with a substrate conversion efficiency of 64.1%.

#### 4. Concluding remarks

*Rhodobacter* sp. KKU-PS1 was isolated from the methane fermentation broth of an UASB reactor. The KKU-PS1 strain efficiently utilized ten carbon sources for hydrogen production. Na-glutamate was a preferred nitrogen source while malic acid was a preferred carbon source for hydrogen production. Initial pH and incubation temperature had a significant effect ( $p \leq 0.05$ ) on H<sub>max</sub> and R<sub>m</sub>, but there were no interaction effects between the initial pH and incubation temperature. Simultaneous maximization of H<sub>max</sub> and R<sub>m</sub> occurred at the optimal initial pH of 7.0, an incubation temperature of 25.6°C and a light intensity of 2500 lx. Under these conditions, maximum H<sub>max</sub> and R<sub>m</sub> values of 1353 mL H<sub>2</sub>/L and 6.8 mL H<sub>2</sub>/L-h were obtained, respectively. Further investigations on the light intensity using the optimum initial pH and incubation temperature indicated that a light intensity of 7500 lx increased R<sub>m</sub> by approximately two fold. Additionally, an increase in illumination intensity shortened the lag phase for hydrogen production.

#### Conflict of interest statement

We have declared no conflict of interest.

#### Financial support

This work was supported by the Thailand Research Fund through the Royal Golden Jubilee Ph.D. Program (Grant No. PHD/0194/2552). Additional acknowledgements go to research funds from the Center for Alternative Energy Research and Development-Khon Kaen University (Grant No. R04/55), the Higher Education Research Promotion and the National Research University Project for Thailand through the Biofuels Research Cluster-Khon Kaen University, Office of the Higher Education Commission.

#### References

- [1] Marbán G, Valdés-Solís T. Towards the hydrogen economy? Int J Hydrog Energy 2007;32:1625–37. <http://dx.doi.org/10.1016/j.ijhydene.2006.12.017>.
- [2] Hay JXW, Wu TY, Juan JC, Jahim JM. Biohydrogen production through photo fermentation or dark fermentation using waste as a substrate: Overview, economics, and future prospects of hydrogen usage. Biofuels Bioprod Biorefin 2013;7:334–52. <http://dx.doi.org/10.1002/bbb.1403>.
- [3] Mudhoo A, Kumar S. Effects of heavy metals as stress factors on anaerobic digestion processes and biogas production from biomass. Int J Environ Sci Technol 2013;10:1383–98. <http://dx.doi.org/10.1007/s13762-012-0167-y>.
- [4] Liu BF, Ren NQ, Xie GJ, Ding J, Guo WQ, Xing DF. Enhanced bio-hydrogen production by the combination of dark- and photo-fermentation in batch culture. Bioresour Technol 2010;101:5325–9. <http://dx.doi.org/10.1016/j.biortech.2010.02.024>.
- [5] Su H, Cheng J, Zhou J, Song W, Cen K. Combination of dark- and photo-fermentation to enhance hydrogen production and energy conversion efficiency. Int J Hydrog Energy 2009;34:8846–53. <http://dx.doi.org/10.1016/j.ijhydene.2009.09.001>.
- [6] Malandra L, Wolfaardt G, Zietsman A, Viljoen-Bloom M. Microbiology of a biological contactor for winery wastewater treatment. Water Res 2003;37:4125–34. <http://dx.doi.org/10.1016/j.memsci.2009.07.013>.
- [7] Lameloise M, Matinier H, Fargues C. Concentration and purification of malate ion from a beverage industry waste water using electro dialysis with homopolar membranes. J Membr Sci 2009;343:73–81. [http://dx.doi.org/10.1016/S0043-1354\(03\)00339-7](http://dx.doi.org/10.1016/S0043-1354(03)00339-7).
- [8] Wu TY, Hay JXW, Kong LB, Juan JC, Jahim JMD. Recent advances in reuse of waste material as substrate to produce biohydrogen by purple non-sulfur (PNS) bacteria. Renew Sustain Energy Rev 2012;16:3117–22. <http://dx.doi.org/10.1016/j.rser.2012.02.002>.
- [9] Laocharoen S, Isolation Reungsang A. Characterization and optimization of photo-hydrogen production conditions by newly isolated *Rhodobacter sphaeroides* KKU-PS5. Int J Hydrog Energy 2014;39:10870–82. <http://dx.doi.org/10.1016/j.ijhydene.2014.05.055>.
- [10] Kim MS, Kim DH, Cha J. Culture conditions affecting H<sub>2</sub> production by phototrophic bacterium *Rhodobacter sphaeroides* KD131. Int J Hydrog Energy 2012;37:14055–61. <http://dx.doi.org/10.1016/j.ijhydene.2012.06.085>.
- [11] Kim DH, Cha J, Kang S, Kim MS. Continuous photo-fermentative hydrogen production from lactate and lactate-rich acidified food waste. Int J Hydrog Energy 2013;38:6161–6. <http://dx.doi.org/10.1016/j.ijhydene.2012.12.072>.
- [12] Akkose S, Gunduz U, Yucel M, Eroglu I. Effects of ammonium ion, acetate and aerobic conditions on hydrogen production and expression levels of nitrogenase genes in *Rhodobacter sphaeroides* O.U.001. Int J Hydrog Energy 2009;34:8818–27. <http://dx.doi.org/10.1016/j.ijhydene.2009.08.040>.
- [13] Chen CY, Lu WB, Wu JF, Chang JS. Enhancing phototrophic hydrogen production of *Rhodospseudomonas palustris* via statistical experiment design. Int J Hydrog Energy 2007;32:940–9. <http://dx.doi.org/10.1016/j.ijhydene.2006.09.021>.
- [14] Shi XY, Yu HQ. Continuous production of hydrogen from mixed volatile fatty acids with *Rhodospseudomonas capsulata*. Int J Hydrog Energy 2006;31:1641–7. <http://dx.doi.org/10.1016/j.ijhydene.2005.12.008>.
- [15] Ozmihi S, Kargi F. Bio-hydrogen production by photo-fermentation of dark fermentation effluent with intermittent feeding and effluent removal. Int J Hydrog Energy 2010;35:6674–80. <http://dx.doi.org/10.1016/j.ijhydene.2010.04.090>.
- [16] Argun H, Kargi F, Kapdan IK. Light fermentation of dark fermentation effluent for bio-hydrogen production by different *Rhodobacter* species at different initial volatile fatty acid (VFA) concentrations. Int J Hydrog Energy 2008;33:7405–12. <http://dx.doi.org/10.1016/j.ijhydene.2008.09.059>.
- [17] Wang YZ, Liao Q, Zhu X, Tian X, Zhang C. Characteristics of hydrogen production and substrate consumption of *Rhodospseudomonas palustris* CQK 01 in an immobilized-cell photobioreactor. Bioresour Technol 2010;101:4034–41. <http://dx.doi.org/10.1016/j.biortech.2010.01.045>.
- [18] Imhoff JF, Hiraiishi A, Su LJ. Anoxygenic phototrophic purple bacteria. In: Brenner DJ, Krieg NR, Staley JT, Garrity GM, editors. Bergey's Manual of Systematic Bacteriology. The Proteobacteria, part A, 2nd ed. New York: Springer-Verlag; 2005. p. 119–32.
- [19] Budiman PM, Wu TY, Ramanan RN, Hay JXW. Treatment and reuse of effluents from palm oil, pulp, and paper mills as a combined substrate by using purple nonsulfur bacteria. Ind Eng Chem Res 2014;53:14921–31. <http://dx.doi.org/10.1021/ie501798f>.
- [20] Belila A, Fazaa I, Hassen A, Ghrabi A. Anoxygenic phototrophic bacterial diversity within wastewater stabilization plant during 'red water' phenomenon. Int J Environ Sci Technol 2013;10:837–46. <http://dx.doi.org/10.1007/s13762-012-0163-2>.
- [21] Basak N, Das D. The prospect of purple non-sulfur (PNS) photosynthetic bacteria for hydrogen production: The presence state of the art. World J Microbiol Biotechnol 2007;23:31–42. <http://dx.doi.org/10.1007/s11274-006-9190-9>.
- [22] Dasgupta CN, Gilbert JJ, Lindblad P, Heidorn T, Borgvang SA, Skjanes K, et al. Recent trends on the development of photobiological processes and photobioreactors for the improvement of hydrogen production. Int J Hydrog Energy 2010;35:10218–38. <http://dx.doi.org/10.1016/j.ijhydene.2010.06.029>.
- [23] Igarashi RY, Seefeldt LC. Nitrogen fixation: The mechanism of the Mo-dependent nitrogenase. Crit Rev Biochem Mol Biol 2003;38:351–84. <http://dx.doi.org/10.1080/10409230390242380>.
- [24] Hu Y, Ribbe MW. Nitrogenase assembly. Biochim Biophys Acta Bioenerg 2013;1827:1112–22. <http://dx.doi.org/10.1016/j.bbabi.2012.12.001>.
- [25] Tan JW, Thong KL, Arumugam ND, Cheah WL, Lai YW, Chua KH, et al. Development of a PCR assay for the detection of *nifH* and *nifD* genes in indigenous photosynthetic bacteria. Int J Hydrog Energy 2009;34:7538–41. <http://dx.doi.org/10.1016/j.ijhydene.2009.04.029>.
- [26] Chen CY, Liu CH, Lo YC, Chang JS. Perspectives on cultivation strategies and photobioreactor designs for photo-fermentative hydrogen production. Bioresour Technol 2011;102:8484–92. <http://dx.doi.org/10.1016/j.biortech.2011.05.082>.
- [27] Akroum-Amrouche D, Abdi N, Lounici H, Mameri N. Effect of physico-chemical parameters on biohydrogen production and growth characteristics by batch culture of *Rhodobacter sphaeroides* CIP 60.6. Appl Energy 2011;88:2130–5. <http://dx.doi.org/10.1016/j.apenergy.2010.12.044>.
- [28] Akkerman I, Janssen M, Rocha J, Wijffels RH. Photobiological hydrogen production: Photochemical efficiency and bioreactor design. Int J Hydrog Energy 2002;27:1195–208. [http://dx.doi.org/10.1016/S0360-3199\(02\)00071-X](http://dx.doi.org/10.1016/S0360-3199(02)00071-X).
- [29] Chen CY, Lee CM, Chang JS. Hydrogen production by indigenous photosynthetic bacterium *Rhodospseudomonas palustris* WP3-5 using optical-fiber-illuminating photobioreactors. Biochem Eng J 2006;32:33–42. <http://dx.doi.org/10.1016/j.bej.2006.08.015>.
- [30] Chen CY, Lee CM, Chang JS. Feasibility study on bioreactor strategies for enhanced photohydrogen production from *Rhodospseudomonas palustris* WP3-5 using optical-fiber-assisted illumination systems. Int J Hydrog Energy 2006;31:2345–55. <http://dx.doi.org/10.1016/j.ijhydene.2006.03.007>.
- [31] Basak N, Jana AK, Das D. Optimization of molecular hydrogen production by *Rhodobacter sphaeroides* O.U.001 in the annular photobioreactor using response surface methodology. Int J Hydrog Energy 2014;39:11889–901. <http://dx.doi.org/10.1016/j.ijhydene.2014.05.108>.
- [32] O-Thong S, Prasertsan P, Intrasingkha N, Dhamwichukorn S, Birkeland NK. Optimization of simultaneous thermophilic fermentative hydrogen production and COD reduction from palm oil mill effluent by *Thermoanaerobacterium-rich* sludge. Int J Hydrog Energy 2008;33:1221–31. <http://dx.doi.org/10.1016/j.ijhydene.2007.12.017>.

- [33] Stanbury PF, Whitaker A, Hall SJ. Principles of Fermentation Technology. 2nd ed. New Delhi, India: Aditya Book (P) Ltd; 1997 93–122.
- [34] Annadurai G, Balan SM, Murugesan T. Box-Behnken design in the development of optimized complex medium for phenol degradation using *Pseudomonas putida* (NICM 2174). *Bioprocess Eng* 1999;21:415–21. <http://dx.doi.org/10.1007/PL00009082>.
- [35] Teh CY, Wu TY, Juan JC. Optimization of agro-industrial wastewater treatment using unmodified rice starch as a natural coagulant. *Ind Crop Prod* 2014;56:17–26. <http://dx.doi.org/10.1016/j.indcrop.2014.02.018>.
- [36] Biehl H, Pfennig N. Isolation of members of the family *Rhodospirillaceae*. In: Starr MP, Stolp H, Trüper HG, Balows A, Schlegel HG, editors. *The Prokaryotes*, vol. 1. New York: Springer; 1981. p. 267–73.
- [37] Edwards T, Rogall T, Blocker H, Emde M, Bottger EC. Isolation and direct complete nucleotide determination of entire genes. Characterization of a gene coding for 16S ribosomal RNA. *Nucleic Acids Res* 1989;17:7843–53. <http://dx.doi.org/10.1093/nar/17.19.7843>.
- [38] Khamtib S, Plangklang P, Reungsang A. Optimization of fermentative of hydrogen production from hydrolysate of microwave assisted sulfuric acid pretreated oil palm trunk by hot spring enriched culture. *Int J Hydrog Energy* 2011;36:14204–16. <http://dx.doi.org/10.1016/j.ijhydene.2011.05.117>.
- [39] Altschul SF, Madden TL, Schaffer AA, Zhang J, Zhang Z, Miller W, et al. Gapped BLAST and PSI-BLAST: A new generation of protein database search programs. *Nucleic Acids Res* 1997;25:3389–402. <http://dx.doi.org/10.1093/nar/25.17.3389>.
- [40] Thompson JD, Gibson TJ, Plewniak F, Jeanmougin F, Higgins DG. The CLUSTAL\_X windows interface: Flexible strategies for multiple sequence alignment aided by quality analysis tools. *Nucleic Acids Res* 1997;25:4876–82. <http://dx.doi.org/10.1093/nar/25.24.4876>.
- [41] Saito N, Nei M. The neighbor-joining method: A new method for reconstructing phylogenetic trees. *Mol Biol Evol* 1987;4:406–25.
- [42] Felsenstein J. Confidence limits on phylogenies: An approach using the bootstrap. *Evolution* 1985;39:783–91. <http://dx.doi.org/10.2307/2408678>.
- [43] Lee JZ, Klaus DM, Maness PC, Spear JR. The effect of butyrate concentration on hydrogen production via photo fermentation for use in a Martian habitat resource recovery process. *Int J Hydrog Energy* 2007;3301–7. <http://dx.doi.org/10.1016/j.ijhydene.2007.05.029>.
- [44] Tao Y, He Y, Wu Y, Liu F, Li X, Zong W, et al. Characteristics of a new photosynthetic bacterial strain for hydrogen production and its application in wastewater treatment. *Int J Hydrog Energy* 2008;33:963–73. <http://dx.doi.org/10.1016/j.ijhydene.2007.11.021>.
- [45] Lazaro CZ, Varesche MBA, Silva EL. Effect of inoculum concentration, pH, light intensity and lighting regime on hydrogen production by phototrophic microbial consortium. *Renew Energy* 2015;75:1–7. <http://dx.doi.org/10.1016/j.renene.2014.09.034>.
- [46] Box GEP, Hunter WG, Hunter JS. *Statistics for Experimenters*. New York: Wiley; 1978.
- [47] Lay JJ. Modeling and optimization of anaerobic digested sludge converting starch to hydrogen. *Biotechnol Bioeng* 2000;68:269–78. [http://dx.doi.org/10.1002/\(SICI\)1097-0290\(20000505\)68:3b269::AID-BIT5N3.0.CO;2-T](http://dx.doi.org/10.1002/(SICI)1097-0290(20000505)68:3b269::AID-BIT5N3.0.CO;2-T).
- [48] Hay JXW, Wu TY, Teh CY, Jahim JM. Optimized growth of *Rhodobacter sphaeroides* O.U.001 using response surface methodology (RSM). *J Sci Ind Res* 2012;71:149–54.
- [49] Bianchi L, Mannelli F, Viti C, Adessi A, Philippis RD. Hydrogen-producing purple non-sulfur bacteria isolated from the trophic lake Averno (Naples, Italy). *Int J Hydrog Energy* 2010;35:12216–23. <http://dx.doi.org/10.1016/j.ijhydene.2010.08.038>.
- [50] Khamtib S, Reungsang A. Biohydrogen production from xylose by *Thermoanaerobacterium thermosaccharolyticum* KKU 19 isolated from hot spring sediment. *Int J Hydrog Energy* 2012;37:12219–28. <http://dx.doi.org/10.1016/j.ijhydene.2012.06.038>.
- [51] Owen WF, Stuckey DC, Healy Jr JB, Young LY, McCarty PL. Bioassay for monitoring biochemical methane potential and anaerobic toxicity. *Water Res* 1979;13:485–92. [http://dx.doi.org/10.1016/0043-1354\(79\)90043-5](http://dx.doi.org/10.1016/0043-1354(79)90043-5).
- [52] Fangkum A, Reungsang A. Biohydrogen production from sugarcane bagasse hydrolysate by elephant dung: Effects of initial pH and substrate concentration. *Int J Hydrog Energy* 2011;36:8687–96. <http://dx.doi.org/10.1016/j.ijhydene.2010.05.119>.
- [53] Saraphrom P, Reungsang A. Biological hydrogen production from sweet sorghum syrup by mixed cultures using an anaerobic sequencing batch reactor (ASBR). *Int J Hydrog Energy* 2011;36:8765–73. <http://dx.doi.org/10.1016/j.ijhydene.2010.08.058>.
- [54] Zheng XJ, Yu HQ. Inhibitory effects of butyrate on biological hydrogen production with mixed anaerobic cultures. *J Environ Manage* 2005;74:65–70. <http://dx.doi.org/10.1016/j.jenvman.2004.08.015>.
- [55] Khanal SK, Chen WH, Li L, Sung S. Biological hydrogen production: Effect of pH and intermediate products. *Int J Hydrog Energy* 2004;29:1123–31. <http://dx.doi.org/10.1016/j.ijhydene.2003.11.002>.
- [56] Zhang H, Bruns MA, Logan BE. Biological hydrogen production by *Clostridium acetobutylicum* in an unsaturated flow reactor. *Water Res* 2006;40:728–34. <http://dx.doi.org/10.1016/j.watres.2005.11.041>.
- [57] Uyar B, Eroglu I, Yucel M, Gunduz U. Photofermentative hydrogen production from volatile fatty acids present in dark fermentation effluents. *Int J Hydrog Energy* 2009;34:4517–23. <http://dx.doi.org/10.1016/j.ijhydene.2008.07.057>.
- [58] Van Niel CB. The culture, general physiology, morphology, and classification of the non-sulfur purple and brown bacteria. *Bacteriol Rev* 1944;8:1–118.
- [59] Imhoff JF. Anoxygenic Photosynthetic Bacteria: Taxonomy and Physiology of Purple Bacteria and Green Sulfur Bacteria. In: Blankenship RE, Madigan MT, Bauer CE, editors. USA: Kluwer Academic Publishers; 1995. p. 1–14.
- [60] Danyal K, Dean DR, Hoffman BM, Seefeldt LC. Electron transfer within nitrogenase: Evidence for a deficit-spending mechanism. *Biochemistry* 2011;50:9255–63. <http://dx.doi.org/10.1021/bi201003a>.
- [61] Seefeldt LC, Yang ZY, Duval S, Dean DR. Nitrogenase reduction of carbon-containing compounds. *Biochim Biophys Acta Bioenerg* 2013;1827:1102–11. <http://dx.doi.org/10.1016/j.bbabi.2013.04.003>.
- [62] Spatzal T, Aksoyoglu M, Zhang L, Andrade SL, Schleicher E, Weber DC, et al. Evidence for interstitial carbon in nitrogenase FeMo cofactor. *Science* 2011;334:940. <http://dx.doi.org/10.1126/science.1214025>.
- [63] Xie GJ, Liu BF, Xing DF, Ding J, Nan J, Ren HY, et al. The kinetic characterization of photofermentative bacterium *Rhodospseudomonas faecalis* RLD-53 and its application for enhancing continuous hydrogen production. *Int J Hydrog Energy* 2012;37:13718–24. <http://dx.doi.org/10.1016/j.ijhydene.2012.02.168>.
- [64] Holt JG, Krieg NR, Sneath PHA, Staley JT. *Bergey's Manual of Determinative Bacteriology*. Baltimore: Williams and Wilkins; 1994.
- [65] Chen CY, Chang JS. Enhancing phototrophic hydrogen production by solid-carrier assisted fermentation and internal optical-fiber illumination. *Process Biochem* 2006;41:2041–9. <http://dx.doi.org/10.1016/j.procbio.2006.05.005>.
- [66] Fang HHP, Liu H, Zhang T. Phototrophic hydrogen production from acetate and butyrate in wastewater. *Int J Hydrog Energy* 2005;30:785–93. <http://dx.doi.org/10.1016/j.ijhydene.2004.12.010>.
- [67] Merugu R, Grisham S, Reddy SM. Bioproduction of hydrogen by *Rhodobacter capsulatus* KU002 isolated from leather industry effluents. *Int J Hydrog Energy* 2010;35:9591–7. <http://dx.doi.org/10.1016/j.ijhydene.2010.06.057>.
- [68] Mongi F, Edward C, William H, Gwang-Hoon G, Almadidy A. Influence of culture parameters on biological hydrogen production by *Clostridium saccharoperbutylacetonicum* ATCC 27021. *World J Microbiol Biotechnol* 2005;21:855–62. <http://dx.doi.org/10.1007/s11274-004-5972-0>.
- [69] Kim MS, Kim DH, Cha J, Lee JK. Effect of carbon and nitrogen sources on photofermentative H<sub>2</sub> production associated with nitrogenase, uptake hydrogenase activity, and PHB accumulation in *Rhodobacter sphaeroides* KD131. *Bioresour Technol* 2012;116:179–83. <http://dx.doi.org/10.1016/j.biortech.2012.04.011>.
- [70] Cai J, Wang G. Hydrogen production by a marine photosynthetic bacterium, *Rhodovulum sulfidophilum* P5, isolated from a shrimp pond. *Int J Hydrog Energy* 2012;37:15070–80. <http://dx.doi.org/10.1016/j.ijhydene.2012.07.130>.
- [71] Wang YZ, Liao Q, Zhu X, Li J, Lee DJ. Effect of culture conditions on the kinetics of hydrogen production by photosynthetic bacteria in batch culture. *Int J Hydrog Energy* 2011;36:14004–13. <http://dx.doi.org/10.1016/j.ijhydene.2011.04.005>.
- [72] Franchi E, Tosi C, Scolla G, Penna GD, Rodríguez F, Pedroni PM. Metabolically engineered *Rhodobacter sphaeroides* RV strains for improved biohydrogen photo production combined with disposal of food wastes. *Mar Biotechnol* 2004;6:552–65. <http://dx.doi.org/10.1007/s10126-004-1007-y>.
- [73] Pandey A, Srivastava N, Sinha P. Optimization of hydrogen production by *Rhodobacter sphaeroides* NMBL-01. *Biomass Bioenergy* 2012;37:251–6. <http://dx.doi.org/10.1016/j.biombioe.2011.12.005>.
- [74] Han H, Liu B, Yang H, Shen J. Effect of carbon sources on the photobiological production of hydrogen using *Rhodobacter sphaeroides* RV. *Int J Hydrog Energy* 2012;37:12167–74. <http://dx.doi.org/10.1016/j.ijhydene.2012.03.134>.
- [75] Basak N, Das D. Photo fermentative hydrogen production using purple non-sulfur bacteria *Rhodobacter sphaeroides* O.U.001 in an annular photobioreactor: A case study. *Biomass Bioenergy* 2009;33:911–9. <http://dx.doi.org/10.1016/j.biombioe.2009.02.007>.
- [76] Suwansaard M, Choorit W, Zeilstra-Ryalls JH, Prasertsan P. Isolation of anoxygenic photosynthetic bacteria from Songkhla Lake for use in a two-staged biohydrogen production process from palm oil mill effluent. *Int J Hydrog Energy* 2009;34:7523–9. <http://dx.doi.org/10.1016/j.ijhydene.2009.05.077>.
- [77] Willison JC, Madern D, Vignais PM. Increased photoproduction of hydrogen by non-autotrophic mutants of *Rhodospseudomonas capsulata*. *Biochem J* 1984;219:593–600.
- [78] Klasson KT, Lundback KMO, Clausen EC, Gaddy JL. Kinetics of light limited growth and biological hydrogen production from carbon monoxide and water by *Rhodospirillum rubrum*. *J Biotechnol* 1993;29:177–88. [http://dx.doi.org/10.1016/0168-1656\(93\)90049-5](http://dx.doi.org/10.1016/0168-1656(93)90049-5).
- [79] Kim NJ, Lee JK, Lee CG. Pigment reduction to improve photosynthetic productivity of *Rhodobacter sphaeroides*. *J Microbiol Biotechnol* 2004;14:442–9.
- [80] Asada Y, Miyake J. Photobiological hydrogen production. *J Biosci Bioeng* 1999;88:1–6. [http://dx.doi.org/10.1016/S1389-1723\(99\)80166-2](http://dx.doi.org/10.1016/S1389-1723(99)80166-2).
- [81] Kim MS, Baek JS, Lee JK. Comparison of H<sub>2</sub> accumulation by *Rhodobacter sphaeroides* KD131 and its uptake hydrogenase and PHB synthase deficient mutant. *Int J Hydrog Energy* 2006;31:121–7. <http://dx.doi.org/10.1016/j.ijhydene.2004.10.023>.
- [82] Kawagoshi Y, Oki Y, Nakano I, Fujimoto A, Takahashi H. Biohydrogen production by isolated halotolerant photosynthetic bacteria using long-wavelength light-emitting diode (LW-LED). *Int J Hydrog Energy* 2010;35:13365–9. <http://dx.doi.org/10.1016/j.ijhydene.2009.11.121>.
- [83] Li X, Wang YH, Zhang SL, Chu J, Zhang M, Huang MZ, et al. Enhancement of phototrophic hydrogen production by *Rhodobacter sphaeroides* ZX-5 using a novel strategy – Shaking and extra-light supplementation approach. *Int J Hydrog Energy* 2009;34:9677–85. <http://dx.doi.org/10.1016/j.ijhydene.2009.10.020>.